

This item was submitted to Loughborough's Institutional Repository (<https://dspace.lboro.ac.uk/>) by the author and is made available under the following Creative Commons Licence conditions.



CC creative commons
COMMONS DEED

Attribution-NonCommercial-NoDerivs 2.5

You are free:

- to copy, distribute, display, and perform the work

Under the following conditions:

BY: **Attribution.** You must attribute the work in the manner specified by the author or licensor.

Noncommercial. You may not use this work for commercial purposes.

No Derivative Works. You may not alter, transform, or build upon this work.

- For any reuse or distribution, you must make clear to others the license terms of this work.
- Any of these conditions can be waived if you get permission from the copyright holder.

Your fair use and other rights are in no way affected by the above.

This is a human-readable summary of the [Legal Code \(the full license\)](#).

[Disclaimer](#) 

For the full text of this licence, please go to:
<http://creativecommons.org/licenses/by-nc-nd/2.5/>

Comparing different approaches for determining joint torque parameters from isovelocity dynamometer measurements

S.E. Forrester¹, M.R. Yeadon², M.A. King² and M.T.G. Pain²

¹ Wolfson School of Mechanical and Manufacturing Engineering, Loughborough University, LE11 3TU, UK

² School of Sport, Exercise and Health Sciences, Loughborough University, LE11 3TU, UK

Abstract

Strength, or maximum joint torque, is a fundamental factor governing human movement, and is regularly assessed for clinical and rehabilitative purposes as well as for research into human performance. This study aimed to identify the most appropriate protocol for fitting a maximum voluntary torque function to experimental joint torque data. Three participants performed maximum isometric and concentric-eccentric knee extension trials on an isovelocity dynamometer and a separate experimental protocol was used to estimate maximum knee extension angular velocity. A nine parameter maximum voluntary torque function, which included angle, angular velocity and neural inhibition effects, was fitted to the experimental torque data and three aspects of this fitting protocol were investigated. Using an independent experimental estimate of maximum knee extension angular velocity gave lower variability in the high concentric velocity region of the maximum torque function compared to using dynamometer measurements alone. A weighted root mean square difference (RMSD) score function, that forced the majority (73 – 92%) of experimental data beneath the maximum torque function, was found to best account for the one-sided noise in experimental torques resulting from sub-maximal effort by the participants. The suggested protocol (an appropriately weighted RMSD score function and an independent estimate of maximum knee extension angular velocity) gave a weighted RMSD of between 11 and 13 Nm (4 – 5% of maximum isometric torque). It is recommended that this protocol be used in generating maximum voluntary joint torque functions in all torque-based modelling of dynamic human movement.

Keywords: maximum velocity knee extension, quadriceps, maximum voluntary joint torque

Introduction

The expression of *in vivo* whole muscle force production is poorly established compared to the *in vitro* equivalent first described by Hill (1938) and Harry et al. (1990). Maximum torque expressed at the joint level is a complex integration of the muscle fibre contractile properties with the *in vivo* architecture of multiple muscle fibres, connective tissue and neural input. Inhomogeneous muscle properties, fibre pennation, series and parallel elastic effects, variability in moment arm and involuntary neural inhibition (Pain and Forrester, 2009) all contribute to differences between the expressed net joint torque–angle–angular velocity profile and the individual muscle force–length–velocity profiles. These features suggest the importance of determining subject-specific strength parameters in the analysis of human movement if accurate representations are to be achieved.

Models of dynamic human movement are based on either individual muscle models, in which each muscle is represented by parameters describing its active, passive and architectural properties, or joint torque generators where all the muscles crossing a joint are lumped together to form a single torque generator. An advantage of the former is that it allows for the modelling of biarticular muscle effects; however parameter values are generally scaled from literature data on cadaver specimens (e.g. van Soest et al., 1993; Jacobs et al., 1996) making model evaluation difficult (Yeadon and Challis, 1994). The second approach

has the advantage of allowing subject-specific torque functions to be readily obtained from maximum torque measurements on an isovelocity dynamometer (Yeadon et al., 2006) and hence model evaluation is more robust; however biarticular effects and antagonist co-activation are not fully accounted for. Regardless, the success of joint torque generators using measured torque functions has been demonstrated for many different activities (Yeadon and King, 2002; Sprigings and Miller, 2004; Mills et al., 2008, Mills et al., 2009; Yeadon et al., 2010). However, challenges exist in obtaining accurate subject-specific torque functions from dynamometer measurements and the development of a more robust protocol for this process would further improve the models of dynamic human movement based on joint torque generators.

Mathematical functions for the variation in maximum voluntary torque with angle and angular velocity have been proposed by Yeadon et al. (2006) and Anderson et al. (2007). The functions are based on adaptations of the established *in vitro* force-length-velocity models and are defined by a number of physiological parameters. Yeadon et al. (2006) included *in vivo* neural inhibition commonly observed for eccentric and low concentric velocities (Westing et al., 1991). In all cases the physiological parameters were determined using experimental torque measurements obtained from isovelocity dynamometer testing. The reliability of measurements obtained from dynamometers requires careful consideration. Actual joint kinematics can deviate substantially from the crank values (Herzog, 1988) necessitating their independent measurement. Direct measurements on *in vivo* and *in vitro* human muscle give maximum shortening velocities of around 6 optimal fibre lengths per second (fl s^{-1}) (Faulkner et al., 1986; Cook & McDonagh 1996; Camilleri & Hull, 2005). Within the muscle modelling literature a wide range of maximum shortening velocities have been applied ranging from 4.4 fl s^{-1} (Alexander, 1995) to 12.7 fl s^{-1} (van Soest et al., 1993). Using representative literature values for knee extensor moment arms and quadriceps fibre lengths (Hoy et al., 1990; Kellis & Baltzopoulos, 1999) and ignoring more complex intramuscular architecture, a dynamometer velocity of 400 deg s^{-1} (typically the maximum) corresponds to a knee extensor velocity of only 3.5 fl s^{-1} . This difference between maximum dynamometer velocity and maximum joint velocity can be problematic in estimating the latter.

These limitations suggest that care is required when fitting a maximum torque function to dynamometer data. This process is further challenged by the inherent nature of the noise in the experimental measurements of strength. Maximum voluntary torque will contain a substantial one-sided noise component since participants can only achieve up to their actual maximum (provided the joint has been appropriately isolated). In this study maximum effort knee extensions were used to investigate three aspects of the function fit with the aim of making global recommendations on the most robust protocol. The three aspects were: (i) Can independent measurements of maximum joint angular velocity provide realistic and useful bounds on this parameter?, (ii) Is it better to fit all parameters in a single stage, or to fit torque-angle and torque-angular velocity parameters in separate stages?, (iii) What is the appropriate weighting of the root mean square difference (RMSD) score function given that actual kinematics can lie either side of experimental kinematics but actual maximum torque can only lie on or above experimental torque?

Methods

Joint torque for maximum effort knee extensions was measured using an isovelocity dynamometer (ISOCOM, Eurokinetics, UK) in order to express torque as a function of joint angle and angular velocity. Three elite athletes (Table 1) participated in the study, which was conducted in accordance with the approval given by Loughborough University Ethical Advisory Committee. Athletic participants were recruited since the development of a robust methodology for fitting a physiologically based strength function to experimental data requires individuals who can consistently perform close to their maximal performance. This

ensured that the experimental data was dominated by the underlying physiological processes and not by the noise associated with the vagaries of untrained human performances.

The athletes were seated on the dynamometer with a hip angle of $125^\circ \pm 5^\circ$. Their dominant leg was strapped tightly to the unpadded crank arm directly above the ankle joint using a moulded plastic shin guard for protection and the rotational axis of the crank arm was aligned with the centre of the knee joint during near-maximal efforts to account for human soft tissue changes. This served to minimise differences between the crank and joint kinematics. An initial gravity correction trial was performed, which involved the relaxed leg being moved through the full range of motion. The protocol involved maximal isometric trials at six knee angles spanning the full range of motion, and maximal isovelocity trials starting at 50°s^{-1} , and increasing in steps of 50°s^{-1} , to a maximum of 400°s^{-1} . The latter employed between two and five repetitions of a concentric-eccentric cycle designed to provide the necessary pre-activation to ensure the middle contractions were maximal (Yeadon et al., 2006). A rest interval of at least two minutes between trials was enforced and a single isometric and dynamic trial was repeated at the end to test for fatigue effects. For one participant these procedures were repeated on a separate day.

Table 1. Participant data and experimentally determined maximum knee extension velocity.

Participant	Age	Height (m)	Mass (kg)	ω_{max} ($^\circ\text{s}^{-1}$)
S1	25	1.83	86.0	1480
S2	22	1.82	72.6	1030
S3	30	1.75	89.3	1610

The output from the dynamometer was used to obtain a maximum voluntary torque–angle–angular velocity dataset. Data were sampled at 1000 Hz and filtered at 8 Hz using a low-pass 4th order zero-lag Butterworth filter. The crank angle and angular velocity were converted to joint angle and angular velocity based on a linear regression of isometric joint angle against crank angle where the former was measured using a mechanical goniometer. For each isometric trial, joint angle and maximum torque were obtained. For each isovelocity trial, the single maximal eccentric phase and the single maximal concentric phase were identified (Figure 1) and the isovelocity plateau defined to be where the velocity was within 10% of the peak value. The isovelocity torques were interpolated using quintic splines (Wood and Jennings, 1979) to give values at 1° intervals.

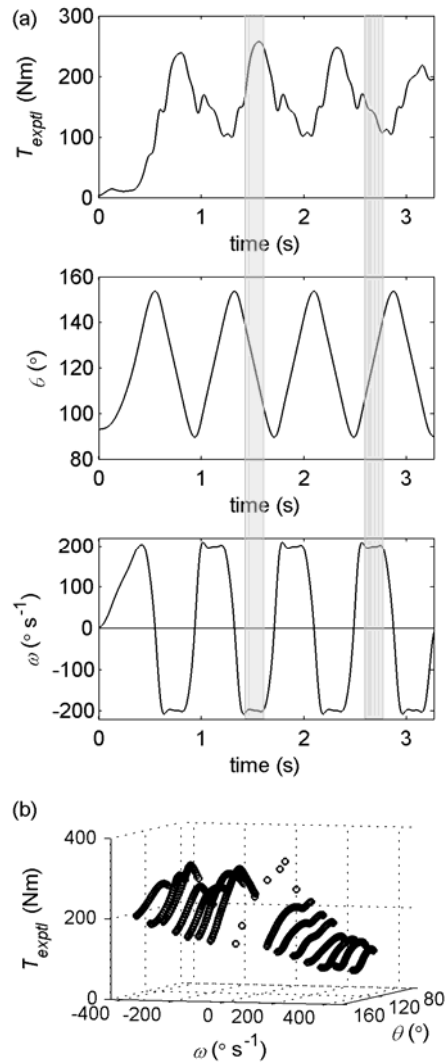


Figure 1. Experimental torque data used to fit the maximum torque function: (a) Raw data from a single dynamometer trial showing torque, angle and angular velocity (200°s^{-1}). The highlighted regions are the selected isovelocity range for the most maximal eccentric and concentric contractions; (b) Torque data from the highlighted regions in (a), showing the complete torque – angle – angular velocity dataset used to fit the maximum torque model. The open circles are from the isometric trials and the closed circles are from the eccentric-concentric trials.

The maximum torque function was defined as the product of tetanic torque–angular velocity, differential activation–angular velocity, and torque–angle functions (Figure 2 and Appendix A). The nine parameters defining maximum torque were obtained using a Simulated Annealing algorithm (Corana et al., 1987) in which the parameter values were varied within bounds (Table 2), in order to minimise a RMSD between the function and experimental torques. To ensure that a global optimum had been found, several independent optimisations were carried out using different initial conditions and different orders for the nine parameters.

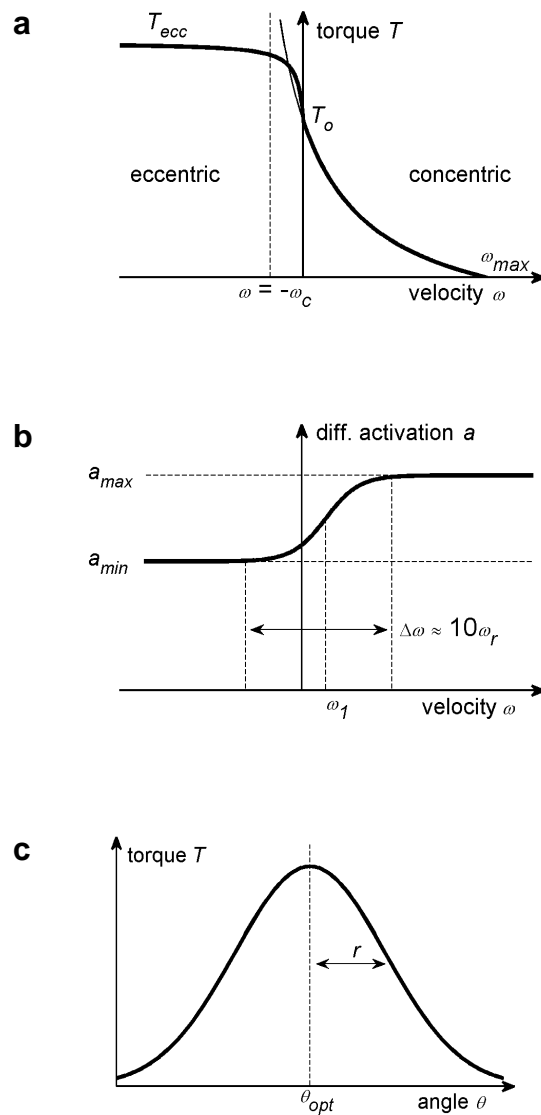


Figure 2. The maximum torque model. (a) Tetanic torque – angular velocity function, comprising a Hill-type hyperbola in the concentric phase and an inverted rectangular hyperbola in the eccentric phase. k is the ratio of slopes between the concentric and eccentric phases and is set to a value of 4.3 representing the theoretical value predicted by Huxley’s (1957) original model. The four parameters are: maximum eccentric torque (T_{ecc}); maximum isometric torque (T_o); maximum angular velocity (ω_{max}); and angular velocity defining the vertical asymptote of the concentric hyperbola (ω_c). (b) Differential activation – angular velocity sigmoid ramp up function. The three parameters are: the low plateau activation level (a_{min}); ω_r which gives the angular velocity range over which the ramp occurs ($\sim 10\omega_r$); and the midpoint angular velocity of the ramp (ω_1). (c) Torque – angle function described by a normal distribution function. The two parameters are: width (standard deviation) of the curve (r); and optimal angle (mean) for torque production (θ_{opt}).

Table 2. Upper and lower bounds on the nine parameters defining the maximum voluntary torque function (see Figure 2 for definition of terms).

Parameter	Bounds	Source
T_{ecc}	$T_{ecc} / T_o = 1.4$	Based on Dudley et al. (1990).
T_o	$T_o \times a_{\omega=0} = T_{o,exptl} \pm 10\%$	Limit the peak maximum voluntary isometric torque to be close to the measured value.
ω_{max}	(i) Experimental measurement: 95% (of individual maximum) → 125% (of group maximum) (ii) Literature: 4.4 – 12.7 optimal fibre lengths per second	(ii) Literature values from Fitts et al. (1989) and Spector et al., (1980). These correspond to $\sim 380 - 2000^\circ\text{s}^{-1}$ for knee extensions based on an optimal fibre length of $80 \text{ mm} \pm 10\%$ (Hoy et al., 1990) and moment arm of $40 \text{ mm} \pm 20\%$ (Kellis and Baltzopoulos, 1999).
ω_c	$\omega_c / \omega_{max} = 0.15 - 0.50$	Pertuzon & Bouisset (1972); Faulkner et al. (1986); Edman (1988).
a_{min}	0.5 – 0.99	Based on the results of EMG activity versus angular velocity measurements during maximal eccentric and concentric knee extensions (Westing et al., 1991; Seger and Thorstensson, 1994).
ω_r	$0 - 90^\circ\text{s}^{-1}$	
ω_l	$\pm 90^\circ\text{s}^{-1}$	
θ_{opt}	Isometric fit value $\pm 5^\circ$	Isometric fit: maximum torque $T_{o,MVC} \geq$ experimental maximum; optimal joint angle $\theta_{t,opt} = 75 - 150^\circ$ for knee extension; width $r = 16^\circ - 52^\circ$ (corresponding to a 90% torque range of motion of between 70° and $220^\circ \sim 0.8 - 1.4$ optimal fibre lengths).
r	Isometric fit value $\pm 5^\circ$	

Three aspects in fitting the maximum torque function to the experimental data were investigated. First, two sets of bounds on maximum joint angular velocity were used, the first based on data from the literature and the second from independent experimental measurements (Table 2). For the latter each participant performed ten isolated maximum velocity knee extensions, five against a soft pad and five into the air. Participants were allowed to stand as they felt comfortable but had to maintain a constant hip angle, measured at $140^\circ \pm 5^\circ$, throughout each trial such that the shank was approximately vertical at maximum velocity. Knee extension angular velocity was recorded using a motion analysis system (Vicon Motion Systems Ltd, Oxford, UK) operating at 500 Hz. Retroreflective markers were positioned on the greater trochanter, lateral femoral epicondyle and lateral malleolus with the raw kinematic data filtered using a 4th order zero-lag Butterworth filter set with a low-pass cut-off of 20 Hz; angular velocity was determined using a first-order finite difference approximation. The three highest angular velocities recorded for each subject were averaged. Bounds on the maximum joint angular velocity parameter were set at 95% of the average value (subject-specific) and 125% of the maximum average value across all the subjects in recognition of errors in kinematic measurements, difficulty in isolation of the knee extensors, and an inability of participants to reach a true maximum velocity.

Second, a 2+7 parameter fit was compared to a 9 parameter fit. The 2+7 parameter fit comprised the determination of the two torque–angle parameters (width and optimal angle) using only the isometric data and then the remaining seven torque–angular velocity parameters using only the isovelocit y data. During the second stage, the two torque–angle parameters were allowed a small amount of leeway ($\pm 5^\circ$) to vary from the isometric optimisation values (Table 2). The 9 parameter fit comprised the determination of all nine parameters using the entire isometric and isovelocit y experimental data in a single stage. In order to achieve this comparison, the correct weighting in the weighted RMSD score function for each of these fits was needed.

Third, different weightings for the RMSD score function were considered, from unweighted to a weighting which forced the majority of the experimental data to lie beneath the surface representing the maximum torque function. Since the actual maximum torque functions for the participants were unknown, this analysis was performed on synthetic data obtained by adding noise to a representative maximum torque–angle–angular velocity function (Figure 3). The noise accounted for two-sided errors in the kinematics and the isometric torques, one set of one-sided errors in the concentric torques close to the edge of the isovelocity region and another set of one-sided errors in all the isovelocity torques. The resulting datasets qualitatively resembled the experimental data collected for the participants in this study (Figure 3e-f).

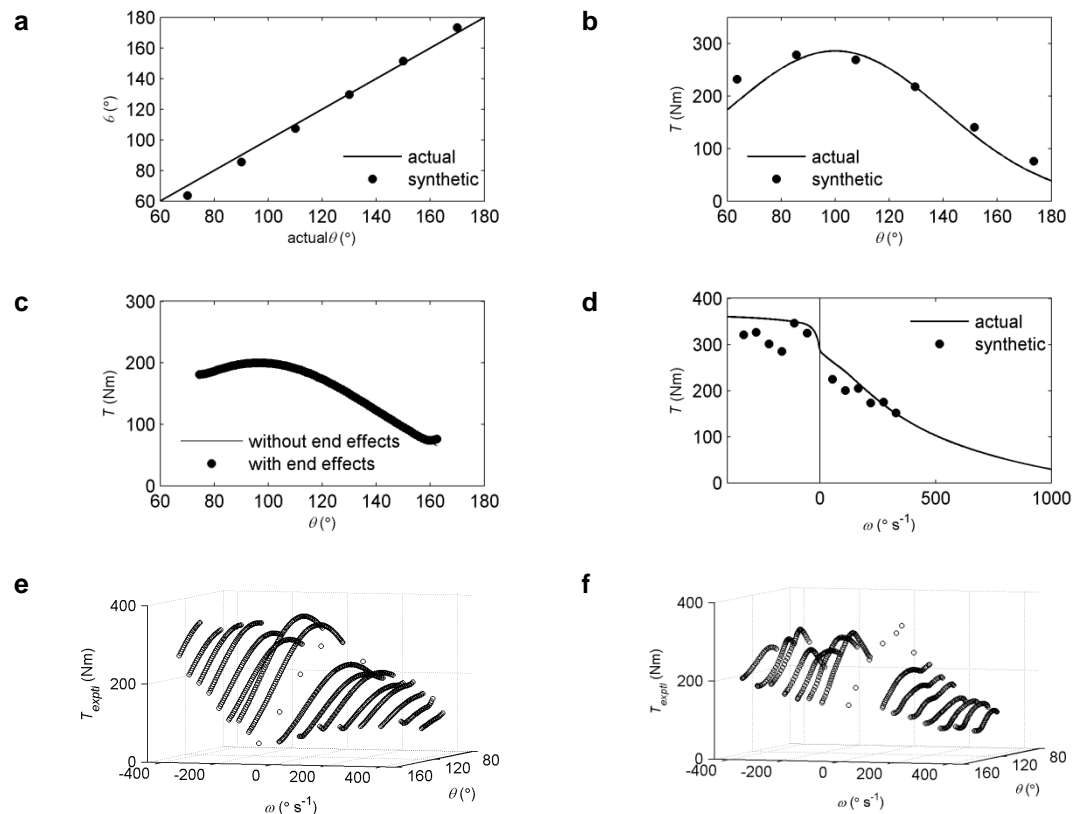


Figure 3. Synthetic dataset construction. (a) Two-sided errors in the isometric goniometer angle versus actual joint angle measurements (absolute error randomly selected from a normal distribution with mean 0° and standard deviation 5°). (b) Two-sided errors in the isometric torque measurements due to submaximal effort by the participant and difficulties in truly isolating the knee extensors under isometric conditions (relative error randomly selected from a normal distribution with mean 1 and standard deviation 0.1). (c) One-sided errors in the concentric isovelocity torque measurements at either end (final 5°) of the isovelocity range of motion due to turnaround effects (absolute error randomly selected from a normal distribution with mean 0 Nm and standard deviation $T_{\max}(\square)$, and multiplied by $\sin(0^\circ \rightarrow 5)$). (d) One-sided errors in the isovelocity torque measurements due to submaximal effort by the participant (relative error randomly selected from the left hand side of a normal distribution with mean 1 and standard deviation 0.15). (e) Complete synthetic dataset. (f) Participant S1 experimental data.

Optimal weightings for the score functions required for the two fitting procedures were investigated. For the 2+7 fitting procedure, different weightings in the RMSD score function for the isometric torque–angle data were assessed to determine the weighting that most closely reproduced the actual optimal angle and width. Thereafter, different weightings in the RMSD score function for the isovelocity torque data were assessed to determine the weighting that best accounted for the one-sided errors due to sub-maximal effort (Figures 3d). For the 9 parameter fit, different weightings in the RMSD score function for the isometric and

isovelocity torque data were assessed to determine the weighting that again best accounted for the one-sided errors due to sub-maximal effort. For each weighting, 1000 sets of synthetic data were fitted and the assessment was based on matching the shape of the residuals distribution between the actual maximum torque surface and synthetic data without one-sided sub-maximal effort noise, and the fitted torque surface and synthetic data with all noise added.

Results

The motion analysis measurements of maximum velocity knee extensions gave angular velocities of between $1030^{\circ}\text{s}^{-1}$ and $1610^{\circ}\text{s}^{-1}$ (Table 1) and provided tighter bounds on maximum knee extension angular velocity compared to the literature data (Table 2). The maximum torque functions obtained from using the two sets of bounds gave very different maximum knee extension angular velocities, e.g. S1, day 1: $1410^{\circ}\text{s}^{-1}$ and $1030^{\circ}\text{s}^{-1}$ (Table 3 and Figure 4) with negligible difference in weighted RMSD score (13 Nm in both cases). The tighter bounds based on the velocity measurements gave more consistent maximum knee extension angular velocities for S1 between days (Table 3 and Figure 4). The highest dynamometer velocity was 400°s^{-1} while the maximum knee extension angular velocities obtained from the fits were in the range $970 - 2000^{\circ}\text{s}^{-1}$.

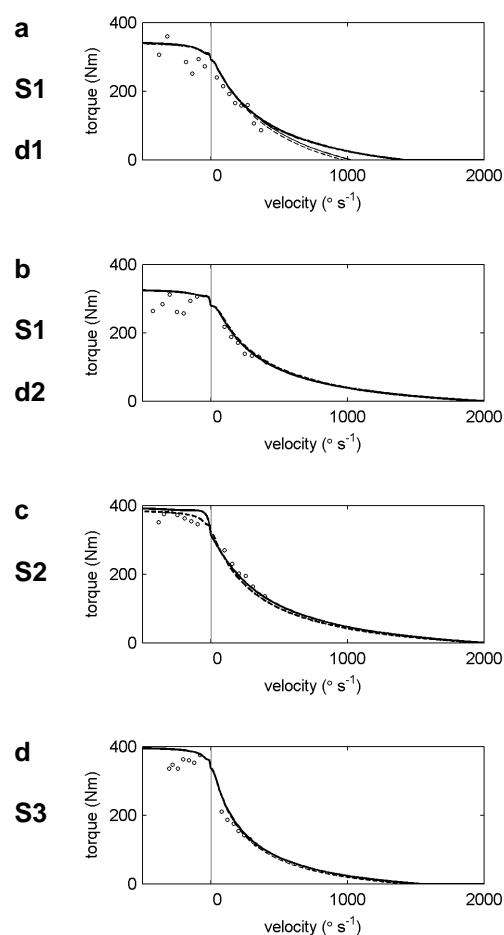


Figure 4. Comparison of the different methods for fitting the maximum torque function to the experimental data. The graphs show maximum torque – angular velocity at optimal angle for: (a) Participant S1 on day 1; (b) Participant S1 on day 2; (c) Participant S2; and (d) Participant S3. The lines represent the maximum torque function and the circles represent the experimental measurements. Thick solid line = 2+7 fit and experimental maximum angular velocity data; thin solid line = 2+7 fit and literature maximum angular velocity data; thick dashed line = 9 fit and experimental maximum angular velocity data; thin dashed line = 9 fit and literature maximum angular velocity data.

Table 3. Maximum torque function parameters for participant S1 from the two testing sessions and from using the different fitting protocols.

(a) day 1					
Fit stages		2+7	2+7	9	9
Max velocity bounds		Exp	Lit	Exp	Lit
	T_o (Nm)	310	308	314	313
$T - \omega$	ω_{max} ($^{\circ}\text{s}^{-1}$)	1410	1030	1410	970
	ω_c ($^{\circ}\text{s}^{-1}$)	396	513	378	473
$a - \omega$	a_{min} (-)	0.796	0.805	0.784	0.788
	ω_r ($^{\circ}\text{s}^{-1}$)	11.8	11.7	13.8	13.8
	ω_l ($^{\circ}\text{s}^{-1}$)	-9.0	-10.1	-8.5	-9.2
$T - \theta$	r ($^{\circ}$)	26.6	26.4	23.9	23.7
	θ_{opt} ($^{\circ}$)	116	116	118	118
Score weighted RMSD (Nm)		13	13	20	20
Equivalent weighted RMSD (Nm)		17	17	17	17

(b) day 2					
Fit stages		2+7	2+7	9	9
Max velocity bounds		Exp	Lit	Exp	Lit
	T_o (Nm)	325	329	329	331
$T - \omega$	ω_{max} ($^{\circ}\text{s}^{-1}$)	2000	1990	2000	2000
	ω_c ($^{\circ}\text{s}^{-1}$)	312	298	321	312
$a - \omega$	a_{min} (-)	0.721	0.713	0.715	0.709
	ω_r ($^{\circ}\text{s}^{-1}$)	21.7	21.8	23.2	23.2
	ω_l ($^{\circ}\text{s}^{-1}$)	1.4	3.0	3.0	4.1
$T - \theta$	r ($^{\circ}$)	38.6	38.0	49.9	48.5
	θ_{opt} ($^{\circ}$)	103	104	92	94
Score weighted RMSD (Nm)		11	11	17	17
Equivalent weighted RMSD (Nm)		14	14	14	14

Notes: The equivalent weighted RMSD has been evaluated for the experimental data and fitted torque function using a weighting mid-way between the values used in the 2+7 fit and 9 fit, in order to allow a more

For the 2+7 parameter fit to the synthetic data, in the isometric stage an unweighted RMSD score function best reproduced the optimal angle and width of the actual torque–angle curve (Table 4). Optimal angle was equally well reproduced by all weightings, but as the weighting increased the width also increased, until actual width was over-predicted by around 6%. In the isovelocity stage, a weighted RMSD score function, which resulted in between

83% and 92% of points lying beneath the fitted function, gave a residuals distribution that best matched that of the synthetic data with added noise (Table 5). For the 9 parameter fit, a weighted RMSD score function, which resulted in between 73% and 85% of points lying beneath the fitted function, gave the best residuals distribution results (Table 5). These weightings were subsequently used in the fits to the subject experimental datasets.

Table 4. Optimal angle and width obtained using different weighted RMSD score functions to fit to synthetic isometric data.

Weighting (% below)	Isometric torque (Nm)	Optimal angle (°)	Width (°)
51 ± 7	348 ± 15	99.7 ± 2.9	40.2 ± 3.0
59 ± 9	350 ± 15	99.7 ± 2.9	40.7 ± 3.0
68 ± 7	353 ± 15	99.7 ± 2.9	40.9 ± 3.0
80 ± 7	364 ± 15	99.9 ± 2.8	41.1 ± 3.0
90 ± 5	383 ± 21	100.1 ± 3.5	41.9 ± 4.1
96 ± 6	385 ± 16	99.5 ± 4.3	42.6 ± 4.3
ACTUAL	350	100	40

Table 5. Residuals distribution parameters obtained using the different weighted RMSD score function to fit the isovelocity data in both the 2+7 fit and the 9 fit. (i) synthetic data (full added noise) and the fitted surface; and (ii) synthetic data (excluding one-sided sub-maximal effort noise) and the actual surface. The highlighted rows indicate the best matching region in skewness and kurtosis between the two conditions.

Weighting (% below)	(i)			(ii)		
	Mean	Skewness	Kurtosis	Mean	Skewness	Kurtosis
2 + 7 fit						
45	-0.0165	-0.49	5.97	0.00434	3.20	27.5
64	0.0205	2.15	22.4	0.00451	3.17	26.4
76	0.0233	3.51	37.6	0.00506	3.00	22.7
83	0.0200	2.97	28.9	0.00583	3.12	21.8
88	0.0175	3.49	34.1	0.00690	3.15	19.5
92	0.0145	3.06	23.1	0.00810	3.21	18.1
97	0.0130	4.11	28.3	0.0112	3.07	15.4
9 fit						
46	-0.0265	-0.779	4.83	0.00419	2.59	18.0
61	0.0251	1.79	17.6	0.00441	2.65	18.1
73	0.0265	2.80	22.4	0.00487	2.77	18.1
80	0.0225	2.27	20.8	0.00538	2.86	18.1
85	0.0185	2.73	24.6	0.00613	3.05	18.9
90	0.0136	1.58	10.2	0.00715	3.21	19.6
95	0.00662	1.26	12.1	0.0103	3.30	18.0

The 2+7 parameter fit gave slightly more consistent results for S1 between days with a RMSD between the two maximum torque functions of 23 Nm (7% of maximum isometric

torque), whilst for the 9 parameter fit this was 32 Nm. Overall, however, there was little difference between the results from these two fitting procedures (Table 3 and Figure 4).

Using the motion analysis data to set bounds on the maximum knee extension angular velocity and applying a 2+7 parameter fit with an unweighted RMSD score function in the first stage and a weighted RMSD score function in the second stage, gave score of between 11 and 13 Nm (Table 6 and Figure 4).

Table 6. Maximum torque function parameters for each participant obtained by fitting to the experimental torque data using the 2+7 fit and the motion analysis data.

Participant		S1 d1	S1 d2	S2	S3
	T_o (Nm)	310	325	335	363
$T - \omega$	ω_{max} ($^{\circ}\text{s}^{-1}$)	1410	2000	2000	1530
	ω_c ($^{\circ}\text{s}^{-1}$)	396	312	385	230
	a_{min} (-)	0.796	0.721	0.848	0.784
$a - \omega$	ω_r ($^{\circ}\text{s}^{-1}$)	11.8	21.7	59.8	9.5
	ω_1 ($^{\circ}\text{s}^{-1}$)	-9.0	1.4	-21.9	-6.0
$T - \theta$	r ($^{\circ}$)	26.6	38.6	33.5	26.5
	θ_{opt} ($^{\circ}$)	116	103	112	135
	Score weighted RMSD (Nm)	13	11	12	12

Notes: d1 refers to the data from the first day of testing for participant S1, and d2 refers to the data from the second day of testing.

Discussion

This study investigated three aspects of fitting a nine-parameter maximum torque function to experimental knee extension torque measurements with the aim of making global recommendations on the most robust protocol. Independent experimental estimates of maximum angular velocity reduced the variability in the high concentric velocity region of the maximum torque function. Fitting the function in either a single stage or two stages gave very similar repeatability of torque parameters. In the two stage fit an unweighted RMSD for the isometric stage and weighted RMSD for the isovelocity stage were found to best account for the one-sided noise in experimental torques due to sub-maximal effort. For S1, the maximum torque functions fitted to the two experimental datasets obtained on different days differed by less than 5%.

The advantage of fitting a maximum torque function to experimental torque measurements is that it allows subject-specific torque to be determined for any combination of angle and angular velocity. Generally it is not possible to obtain dynamometer measurements over the full range of angles and velocities required in subsequent application, hence it is important that the range of measurements is maximised and that extrapolation beyond this range is accurate. Some extrapolation may be justified since the model has a physiological basis: for example, torque is known to approximately plateau with an increase in lengthening velocity (Westing et al., 1988). However, during fibre shortening torque can change rapidly with

velocity, potentially leading to substantial extrapolation errors. The inclusion of a subject-specific experimental estimate of maximum joint velocity from a separate test protocol eliminated this extrapolation and generated an optimised set of parameters far less sensitive to noise in the experimental torque data.

Motion analysis measurements were used to obtain bounds on maximum knee extension velocity. It may be questioned how closely the actual maximum knee extension velocity can be estimated using the described protocol. All of the measured velocities lay within the literature range however the value for S2 was at least 25% lower than the value for the remaining two participants. Initially subject-specific upper and lower bounds were applied. However S1 and S2 were less practised at kicking, had lower maximum velocities and their fits consistently hit their upper bounds, most likely due to an inability to achieve maximum kicking performance. Hence it was decided to switch to a group maximum velocity for setting the upper bound. Only S3 practised kicking as part of his training, was therefore the most experienced, and produced the highest velocities which were used to set the upper bound for all participants. It may be that some practice is required for participants to produce a maximum velocity that is close to their theoretical limit.

The difficulties associated with eliciting consistent maximum voluntary contractions from human participants are well documented (e.g. Clarys and Cabri, 1993). Hence, when attempting to model maximum voluntary torque based on *in vivo* measurements a method of accounting for this inconsistency in effort by the participant is critical. The method applied here was to use a weighted RMSD score function with an optimal weighting determined that best accounted for the noise introduced through sub-maximal effort. This resulted in a weighting that forced the majority (between 73 and 92%) of the experimental data beneath the fitted strength surface. Earlier strength models which use an unweighted RMSD score function (Yeadon et al., 2006; Anderson et al., 2007) risk underestimating the participant's actual strength which may have consequences if subsequently applied in a simulation model of human movement.

Torque can also change rapidly with angle, hence the importance of maximising the measurement range of motion. Due to the acceleration–isovelocity–deceleration profile of the crank arm, isovelocity range is greatest at low velocities and decreases with an increase in velocity (dropping about one third on increasing from 50°s^{-1} to 400°s^{-1}). Thus with an increase in concentric velocity, end-effects noise observed at either end of the isovelocity range (i.e. an upturn in torque) influences a greater proportion of the data. This noise has the potential to influence a fitting procedure which forces the majority of the experimental data beneath the surface. Hence, in addition to a single stage (9 fit) procedure in which all nine parameters were fitted together, a two-stage (2+7 fit) procedure was also considered in which the optimal angle and width of the torque–angle curve were obtained first using the isometric measurements and thereafter the torque–angular velocity parameters were obtained using the dynamic measurements. The latter was thought to have better potential in coping with end-effects noise; however the present results indicated negligible difference in fitting performance between the procedures.

A number of limitations of the current approach can be identified. The selection of athletic subjects was done to ensure that the underlying physiological processes dominated the fitting process rather than noise resulting from the inability to consistently perform close to maximal. A larger group of athletic subjects would further validate the proposed methodology; however there was sufficient inter-subject variability in the experimental data of the participants selected to have confidence in the methodology presented. Some degree of antagonist co-activation will have been present during the dynamometer testing; however for athletic individuals EMG measurements have indicated that this would have been low (≤ 0.1 of MVC; Forrester and Pain, 2010) corresponding to knee flexor torques in the range 5 – 15 Nm (Kellis and Baltzopoulos, 1997). Even at the highest concentric velocities this represents

only approximately 5 – 15% of the measured net extensor torques, and <5% throughout most of the angle-velocity range. Where higher levels of co-contraction are expected, then it may be necessary to include a co-contraction scaling factor within the strength function. The experimental isometric torque measurements consistently sat above the fitted strength function, which is a common observation in strength testing. The fitting procedure accounted for this in the bounds set for maximum isometric torque from the isometric data. Passive mechanical properties have been neglected since they would have had minimal effect over the knee extension range of motion used in this study (Silder et al., 2007).

There are inherent difficulties in subjects achieving maximal effort across a range of joint angular velocities, which results in datasets containing some sub-maximal torques. Literature values for maximum joint angular velocities vary widely and provide little guidance for a specific individual. To overcome such limitations it is recommended that an appropriately weighted RMSD score is used to fit a strength function to experimental torque data and that an independent estimate of maximum joint velocity is included. Such a protocol can be used to generate the maximum voluntary torque function parameter set for use in torque-based modelling of dynamic human movement.

References

- Alexander, R.M., 1995. Leg design and jumping technique for humans, other vertebrates and insects. *Philosophical Transactions of the Royal Society of London. Series B: Biological Sciences* 347, 235–248.
- Anderson, D.E., Madigan, M.L., Nussbaum, M.A., 2007. Maximum voluntary joint torque as a function of joint angle and angular velocity: Model development and application to the lower limb. *Journal of Biomechanics* 40, 3105–3113.
- Camilleri, M.J., Hull, M.L., 2005. Are the maximum shortening velocity and the shape parameter in a Hill-type model of whole muscle related to activation? *Journal of Biomechanics* 38, 2172–2180.
- Clarys, J., Cabri, J., 1993. Electromyography and the study of sports movements: A review. *Journal of Sports Sciences* 11, 379–448.
- Cook, C.S., McDonagh, M.J., 1996. Force responses to constant-velocity shortening of electrically stimulated human muscle-tendon complex. *Journal of Applied Physiology* 81, 384–392.
- Corana, A., Marchesi, M., Martini, C., Ridella, S., 1987. Minimizing multimodal functions of continuous variables with the "simulated annealing" algorithm. *ACM Transactions on Mathematical Software* 13, 262–280.
- Dudley, G.A., Harris, R.T., Duvoisin, M.R., Hather, B.M., Buchanan, P., 1990. Effect of voluntary vs. artificial activation on the relationship of muscle torque to speed. *Journal of Applied Physiology* 69, 2215–2221.
- Edman, K.A.P., 1988. Double-hyperbolic force-velocity relation in frog muscle fibres. *Journal of Physiology* 404, 301–321.
- Faulkner, J.A., Clafin, D.R., McCully, K.K., 1986. Power output of fast and slow fibers from human skeletal muscles. In: N.L. Jones, N. McCartney, A.J. McComas, Editors. *Human Muscle Power*. Human Kinetics Publishers, Inc, Champaign, IL, 81–94.
- Fitts, R.H., Costill, D.L., Gardetto, P.R., 1989. Effect of swim exercise on human muscle fiber function. *Journal of Applied Physiology* 66, 465–475.
- Forrester S.E., Pain M.T.G., 2010. A Combined Muscle Model and Wavelet Approach to Interpreting the Surface EMG Signals From Maximal Dynamic Knee Extensions. *Journal of Applied Biomechanics* 26, 62–72.
- Harry, J.D., Ward, A.W., Heglund, N.C., Morgan, D.L., McMahon, T.A., 1990. Cross-bridge cycling theories cannot explain high-speed lengthening behavior in frog muscle. *Biophysical Society Journal* 57(2), 201–208.

- Herzog, W., 1988. The relationship between the resultant moments at a joint and the moments measured by an isokinetic dynamometer. *Journal of Biomechanics* 21(1), 5–12.
- Hill, A.V., 1938. The heat of shortening and the dynamic constraints of muscle. *Proceedings of the Royal Society of London, Series B* 126, 136–195.
- Hoy, M.G., Zajac, F.E., Gordon, M.E., 1990. A musculoskeletal model of the human lower extremity: The effect of muscle, tendon, and moment arm on the moment-angle relationship of musculotendon actuators at the hip, knee, and ankle. *Journal of Biomechanics* 23(2), 157–169.
- Huxley, A.F., 1957. Muscle structure and theories of contraction. *Progress in Biophysics and Biophysical Chemistry* 7, 225–318.
- Jacobs R., Bobbert M.F., van Ingen Schenau G.J., 1996. Mechanical Output from Individual Muscles during Explosive Extensions: The role of biarticular muscles. *Journal of Biomechanics* 29, 513–523.
- Kellis, E., Baltzopoulos, V., 1999. In vivo determination of the patella tendon and hamstrings moment arms in adult males using videofluoroscopy during submaximal knee extension and flexion. *Clinical Biomechanics* 14, 118–124.
- Kellis E., Baltzopoulos V., 1997. The effects of antagonist moment on the resultant knee joint moment during isokinetic testing of the knee extensors. *European Journal of Applied Physiology* 76, 253–259.
- Mills, C., Pain, M.T.G., Yeadon, M.R., 2008. The influence of simulation model complexity on the estimation of internal loading in gymnastics landings. *Journal of Biomechanics* 41(3), 620–628.
- Mills, C., Pain, M.T.G., Yeadon, M.R., 2009. Reducing ground reaction forces in gymnastics' landings may increase internal loading. *Journal of Biomechanics* 42, 671–678.
- Pain, M.T.G., Forrester, S.E., 2009. Predicting maximum eccentric strength from surface EMG measurements. *Journal of Biomechanics* 42, 1598–1603.
- Pertuzon, E., Bouisset, S., 1972. Biomechanics of monoarticulated movement and mechanical properties of muscle. *Le Travail Humain* 35, 364.
- Seger, J.Y., Thorstensson, A., 1994. Muscle strength and myoelectric activity in prepubertal and adult males and females. *European Journal of Applied Physiology and Occupational Physiology* 69(1), 81–87.
- Silder A., Whittingham B., Heiderscheid B., Thelan D.G., 2007. Identification of passive elastic joint moment–angle relationships in the lower extremity. *Journal of Biomechanics* 40, 2628–2635.
- Spector, S.A., Gardiner, P.F., Zernicke, R.F., Roy, R.R., Edgerton, V.R., 1980. Muscle architecture and force-velocity characteristics of cat soleus and medial gastrocnemius: implications for motor control. *Journal of Neurophysiology* 44, 951–960.
- Springs E.J., Miller D.I., 2004. Optimal knee in springboard extension timing and platform dives from the reverse group. *Journal of Applied Biomechanics* 20, 275–290.
- van Soest, A.J., Schwab, A.L., Bobbert, M.F., van Ingen Schenau, G.J., 1993. The influence of the biarticularity of the gastrocnemius muscle on vertical-jumping achievement. *Journal of Biomechanics* 26, 1–8.
- Westing, S.H., Cresswell, A.G., Thorstensson, A., 1991. Muscle activation during maximal voluntary eccentric and concentric knee extension. *European Journal of Applied Physiology and Occupational Physiology* 62, 104–108.
- Westing, S.H., Seger, J.Y., Karlson, E. & Ekblom, B., 1988. Eccentric and concentric torque-velocity characteristics of the quadriceps femoris in man. *European Journal of Applied Physiology* 58, 100–104.
- Wood, G.A., Jennings, L.S., 1979. On the use of spline functions in data smoothing. *Journal of Biomechanics* 12, 477–479.

- Yeadon M.R., Challis J.H., 1994. The Future of Performance-Related Sports Biomechanics Research. *Journal of Sports Sciences* 12, 3–32.
- Yeadon, M.R., King, M.A., 2002. Evaluation of a torque-driven simulation model of tumbling. *Journal of Applied Biomechanics* 18, 195–206.
- Yeadon, M.R., King, M.A., Wilson, C., 2006. Modelling the maximum voluntary joint torque/angular velocity relationship in human movement. *Journal of Biomechanics* 39, 476–482.
- Yeadon M.R., King M.A., Forrester S.E., Caldwell G.E., Pain M.T.G., 2010. The need for muscle co-contraction prior to a landing. *Journal of Biomechanics* 43, 364–369.

APPENDIX A. NINE PARAMETER MAXIMUM STRENGTH FUNCTION EQUATIONS

Tetanic torque – angular velocity (Figure 2a; Yeadon et al., 2006)

Concentric ($\omega \geq 0$):

$$T = \frac{C}{(\omega_c + \omega)} - T_C \quad \text{where} \quad T_C = \frac{T_o \omega_c}{\omega_{max}}, \quad C = T_C(\omega_{max} + \omega_c)$$

Eccentric ($\omega < 0$):

$$T = \frac{E}{(\omega_E - \omega)} + T_{ecc} \quad \text{where} \quad \omega_E = \frac{(T_{ecc} - T_o)}{kT_o} \frac{\omega_{max} \omega_c}{(\omega_{max} + \omega_c)}, \quad E = -(T_{ecc} - T_o)\omega_E$$

Differential activation – angular velocity (Figure 2b):

$$a = a_{min} + \frac{(a_{max} - a_{min})}{\left[1 + \exp\left(\frac{-(\omega - \omega_1)}{\omega_r}\right) \right]}$$

Torque – angle (Figure 2c; Audu & Davy, 1985):

$$\frac{T(\theta)}{T(\theta_{opt})} = \exp\left[\frac{-(\theta_{opt} - \theta)^2}{2r^2}\right]$$

Additional Reference

Audu, M.L., Davy, D.T., 1985. The influence of muscle model complexity in musculoskeletal motion modeling. *Journal of Biomechanical Engineering* 107, 147–157.